JVI Journals.ASM.org

Rab18 Facilitates Dengue Virus Infection by Targeting Fatty Acid Synthase to Sites of Viral Replication

Wei-Chun Tang,[a,b] Ren-Jye Lin,[c,d] Ching-Len Liao,[a] Yi-Ling Lin[a,b,e]

Graduate Institute of Life Sciences, National Defense Medical Center, Taipei, Taiwan[a]; Institute of Biomedical Sciences, Academia Sinica, Taipei, Taiwan[b]; Department of General Medicine, School of Medicine, College of Medicine, Taipei Medical University, Taipei, Taiwan[c]; Department of Primary Care Medicine, Taipei Medical University Hospital, Taipei, Taiwan[d]; and Genomic Research Center, Academia Sinica, Taipei, Taiwan[e]

ABSTRACT

Positive-sense RNA viruses, such as dengue virus (DENV), hijack the intracellular membrane machinery for their own replication. The Rab18 protein, a member of the Rab GTPase family, key regulators of membrane trafficking, is located on the organelles involved in DENV infection, such as the endoplasmic reticulum (ER) and lipid droplets (LDs). In this study, we addressed the potential involvement of Rab18 in DENV infection by using cells overexpressing the wild-type, GTP-bound active form, or GDP-bound inactive form of Rab18 and cells with Rab18 knockdown. DENV replication, measured by viral protein, viral RNA, and viral progeny production, as well as LD induction, was reduced in cells with inactive Rab18 and in cells deprived of Rab18 expression, suggesting a positive role of Rab18 in the DENV life cycle. Interestingly, the interaction of fatty acid synthase (FASN), a key lipogenic enzyme in lipid biosynthesis, with DENV NS3 protein relied on the conversion of the GDP-bound to the GTP-bound form of Rab18. Furthermore, the targeting of FASN to sites participating in DENV infection, such as the ER and LDs, depends on functional Rab18. Thus, Rab18-mediated membrane trafficking of FASN and NS3 facilitates DENV replication, probably by ensuring a sufficient and coordinated lipid supply for membrane proliferation and arrangement.

IMPORTANCE

Infection by dengue virus (DENV), an important mosquito-borne virus threatening ~40% of the world's population, can cause mild dengue fever or severe dengue hemorrhagic fever and dengue shock syndrome. The pathogenesis mechanisms of DENV-related diseases are not clear, but high viral replication is believed to be a risk factor for the severe form of DENV infection. Thus, understanding the detailed mechanism of DENV replication might help address this devastating virus. Here, we found that Rab18, a small GTPase involved in vesicle trafficking and located in the endoplasmic reticulum network and on the surfaces of lipid droplets, positively regulates DENV replication. The functional machinery of Rab18 is required to recruit the enzyme fatty acid synthase to sites of DENV replication and to interact with DENV NS3 protein to promote fatty acid biosynthesis. Thus, DENV usurps Rab18 to facilitate its own replication.

Dengue virus (DENV), a member of the genus *Flavivirus* of the family *Flaviviridae*, is the causative agent of dengue fever, dengue hemorrhagic fever, and dengue shock syndrome (1). Other members of the family, such as hepatitis C virus (HCV), yellow fever virus, West Nile virus, and Japanese encephalitis virus, are also involved in human diseases. DENV is enveloped and contains a single-stranded positive-sense RNA genome. Like other positive-sense RNA viruses, DENV modifies host cytoplasmic membranes to form platforms for viral replication (2, 3). DENV replication occurs in close association with virus-induced membrane structures derived from the endoplasmic reticulum (ER) network, with spatial coupling between sites of viral replication and virion assembly (4). The membrane rearrangement induced in DENV-infected cells is linked to a unique lipid profile, with an example in mosquito cells in which 85% of the lipid metabolites in the membrane fraction enriched in viral replication components differ from those in the membranes of mock-infected cells (5).

Lipid biogenesis is involved in various steps of DENV infection, such as viral replication, assembly, and energy supply. DENV replicon gene expression and viral progeny production were reduced by knockdown of fatty acid synthase (FASN) and by treatment with cerulenin and C75, 2 inhibitors targeting FASN (6). FASN, a multifunctional protein whose main function is to synthesize long-chain fatty acid by using acetyl-coenzyme A (CoA) and malonyl-CoA (7), is redistributed to sites of DENV replication by binding with DENV nonstructural protein 3 (NS3) to increase cellular fatty acid synthesis (6). FASN enzyme activity was involved in DENV type 2 (DENV-2)-triggered lipid droplet (LD) induction (8); FASN inhibitor C75 treatment reduced the level of LDs and had a profound effect on DENV assembly and progeny production (8). LDs can function as the energy source for enhanced DENV replication during autophagy processing (9). Thus, DENV uses cellular lipids and downstream signaling to facilitate various steps of viral infection.

Ras-related proteins in brain (Rab) GTPases are molecular switches that cycle between a cytosolic GDP-bound inactive form and a membrane-associated GTP-bound active form to regulate membrane trafficking (10). LDs are ER-derived organelles containing a core of neutral lipids enclosed by a monolayer of phos-

Received 7 January 2014 **Accepted** 25 March 2014
Published ahead of print 2 April 2014
Editor: M. S. Diamond
Address correspondence to Yi-Ling Lin, yll@ibms.sinica.edu.tw.

doi:10.1128/JVI.00045-14

pholipids and associated proteins. It is increasingly recognized that LDs interact with other organelles and perform functions beyond lipid storage (11–13). Rab18 is a member of the Rab GTPase family that localizes to LDs and induces close apposition of LDs to membrane cisternae connected to the ER (14, 15). Rab18 is involved in insulin-mediated lipogenesis and in β-adrenergic-induced lipolysis by facilitating the interaction of LDs with the ER membrane and the exchange of lipids between these compartments (16). Besides localizing on LDs, Rab18 also localizes to the Golgi complex, ER, cytosol, and secretory granules of various cell types. Rab18 has other functions, such as inhibition of secretory activity by impairing secretory granule transport (17) and by disrupting ER-Golgi apparatus trafficking (18). Thus, Rab18 is a small GTPase located on cellular organelles known to participate in the DENV life cycle; however, its role in DENV infection has not been illustrated.

In this study, we addressed the potential role of Rab18 in DENV infection by using cells expressing a wild-type (WT) form of Rab18 or mutated Rab18–S22N, which is deficient in GTP binding, thus remaining GDP bound and dominant negative, and Rab18–Q67L, which is unable to hydrolyze GTP, therefore remaining GTP bound and constitutively active (19), as well as cells with Rab18 knockdown. Rab18 appears to play a positive role in LD induction and in the formation of the viral replication complex in DENV-infected cells. Specifically, the interaction of DENV NS3 with FASN and targeting of FASN to sites of DENV replication (6) depend on the proper functioning of Rab18.

MATERIALS AND METHODS

Plasmid constructs. The human Rab18 cDNA (NM_021252) was PCR amplified from A549 cells using the primer pair sequences 5′-ATGGACG AGGACGTGCTAAC-3′ and 5′-TTATAACACAGAGCAATAACCAC C-3′ and fused in frame to the C terminus of mCherry (the mCherry plasmid was kindly provided by Roger Y. Tsien, University of California, San Diego, CA, USA) to establish the mCherry-fused Rab18 WT-expressing plasmid. The GDP-bound inactive form Rab18–S22N and the GTP-bound active form Rab18–Q67L were generated by using the single-primer mutagenesis method (20) with the primer sequences (mutations are underlined) 5′-GAGAGTGGGGTGGGCAAGAACAGCCTGCTCTT GAGGTTCA-3′ and 5′-GCAATATGGGATACTGCTGGTCTAGAGAG GTTTAGAACATTAACTCCCA-3′, respectively. These mCherry-fused Rab18 proteins (WT, Q67L, and S22N) and mCherry were fused in frame with the hemagglutinin (HA) tag of pcDNA3 HA-N1 (21) and then subcloned into pAS4w.1.Phyg (Taiwan National RNAi Core Facility) for lentivirus production. The pCR3.1 vector expressing Flag-tagged DENV-2 NS2B3 has been described previously (22). The lentivirus vectors carrying the short hairpin RNAs (shRNAs) targeting human Rab18 (TRCN0000021979, 5′-GC ACGAAAGCATTCCATGTTA-3′; TRCN0000021980, 5′-GAACATTAACT CCCAGCTATT-3′; TRCN0000021981, 5′-CGTGAAGTCGATAGAAATG AA-3′; TRCN0000021982, 5′-TGGTGGTTATTGCTCTGTGTT-3′; and TRCN0000021983, 5′-CACAGGGTGTTATATTAGTTT-3′) and LacZ (TRCN0000072223, 5′-TGTTCGCATTATCCGAACCAT-3′) were from the Taiwan National RNAi Core Facility. The shRab18-resistant Rab18 was generated on mCherry-Rab18-WT by using the single-primer mutagenesis method (20) with the primer sequences 5′-AATGAAGGCCTG AAATTTGCGCGCAAACACAGCATGCTATTTATAGAGGCAAGTGC AAAAAC-3′ and 5′-GAAATAAAATCGATAAGGAAAATCGAGAGGT CGACCGAAACGAGGGCCTGAAATTTGCACGAA-3′ (mutations are underlined), conferring resistance to shRNAs TRCN0000021979 and TRCN0000021981, respectively.

Virus and cell lines. DENV-2 strain PL046 (23) was propagated in mosquito C6/36 cells, which were grown in RPMI 1640 medium containing 5% fetal bovine serum (FBS). For viral infection, DENV-2 was adsorbed to cells at the indicated multiplicity of infection (MOI) for 2 h at 37°C, and then the unbound virus was removed by a gentle wash with Hanks balanced salt solution (HBSS) (HyClone). At the indicated times postinfection, the culture supernatants were collected and sequentially diluted for plaque-forming assays on BHK-21 cells, as previously described (23). Human lung epithelial carcinoma A549 cells, previously used for DENV study (21, 24), were maintained in F-12 medium (Invitrogen) supplemented with 10% FBS. A549 with *aOn* TRE transactivator and A549 cell lines were used for Rab18 overexpression and Rab18 knockdown, respectively, by lentivirus transduction. Briefly, lentivirus was prepared by cotransfection of the lentiviral vector with helper plasmids, pCMVΔR8.91 and pMD.G, into HEK293/T17 cells using Lipofectamine 2000 (Invitrogen), as described previously (24). Cells were selected with 500 μg/ml hygromycin (InvivoGen) for Rab18 overexpression and with 10 μg/ml puromycin (InvivoGen) for Rab18 knockdown. The cells with mCherry expression were sorted through a FACSAria cell sorter (BD Biosciences) by our Flow Cytometry Core Facility (Academia Sinica, Taiwan) to collect cells with similar fluorescent signals. The fluorescent signal was verified by LSR II flow cytometry (BD Biosciences) and analyzed by FlowJo software v9 (Tree Star).

Immunofluorescence analysis. Cells seeded on coverslips were fixed with 4% paraformaldehyde in phosphate-buffered saline (PBS) for 20 min at room temperature and then washed twice with PBS. The cells were permeabilized in PBS containing 0.1% Triton X-100 (8) and blocked with 1.5% bovine serum albumin (Sigma-Aldrich) in PBS. The primary antibodies anti-calreticulin (Abcam; ab14234), anti-GM130 (BD Biosciences; 610823), anti-FASN (Abcam; ab22759), anti-Rab18 (Sigma-Aldrich; SAB4200173), and anti-DENV-2 NS3 (23) diluted in Tris-buffered saline (TBS) were added for 2 h at room temperature before washing with TBS and then incubated with the proper Alexa Fluor-conjugated secondary antibodies (Alexa Fluor 405 goat anti-mouse [A31553], Alexa Fluor 405 goat anti-rabbit [A31556], Alexa Fluor 568 goat anti-rabbit [A11036], Alexa Fluor 594 goat anti-chicken [A11042], Alexa Fluor 647 goat anti-mouse [A21236], and Alexa Fluor 647 goat anti-chicken [A21449] from Molecular Probes) for 1 h at room temperature. For LD staining, 2 μg/ml Bodipy 493/503 (Invitrogen; D-3922) was added during the secondary-antibody staining. The number of LDs was determined as the objects with pixel intensity greater than the background intensity in the fluorescein isothiocyanate (FITC) channel with cell edges defined by the mCherry signal, using MetaMorph v7.6.5.0 (Molecular Devices). For mitochondrial staining, 100 ng/ml of MitoTracker Green FM (Invitrogen; M-7514) was added to the serum-free medium 30 min before fixation. After washing, the coverslips were mounted on slides using ProLong Gold Antifade Reagent (Life Technologies; P36934). The cells were observed and photographed under a Zeiss LSM510 Meta Confocal Microscope with a 63× objective, 1.4 numerical aperture (NA) (Zeiss), and *z*-axis size of 0.7 μm. The visualization of colocalization and calculation of the colocalization coefficient were performed by using the ZEN 2011 software (Zeiss) colocalization module. To exclude the possibility that no colocalization was due to low expression, Pearson's correlation coefficient (PCC) analysis for the colocalization coefficient was performed using Volocity 6.3 software (Perkin Elmer) to analyze the signals of mCherry-Rab18-WT, -S22N, and -Q67L with different expression levels.

Immunoprecipitation (IP) and Western blot analysis. HEK293T/17 cells were transfected with the indicated plasmids using Lipofectamine 2000 for 48 h. After a wash with PBS, the cells were lysed in protein lysis buffer (10 mM Tris, pH 7.2, 150 mM NaCl, 5 mM EDTA, 1% sodium deoxycholate, 0.1% SDS, and 1% Triton X-100) containing the Complete protease inhibitor cocktail (Roche) and homogenized by sonication (VCX600; Sonics & Materials, Inc.). The cell lysates were immunoprecipitated with anti-HA affinity gel (Sigma; E6779), anti-Flag M2 affinity gel (Sigma; A2220), or mouse IgG-agarose (Sigma; A0919) on a rotator (ELMI RM-2L; 30 rpm) for 12 h at 4°C. The proteins were eluted with HA or Flag peptides for 15 min at room temperature. The eluted proteins were separated by 10% SDS-PAGE and transferred to polyvinylidene difluoride

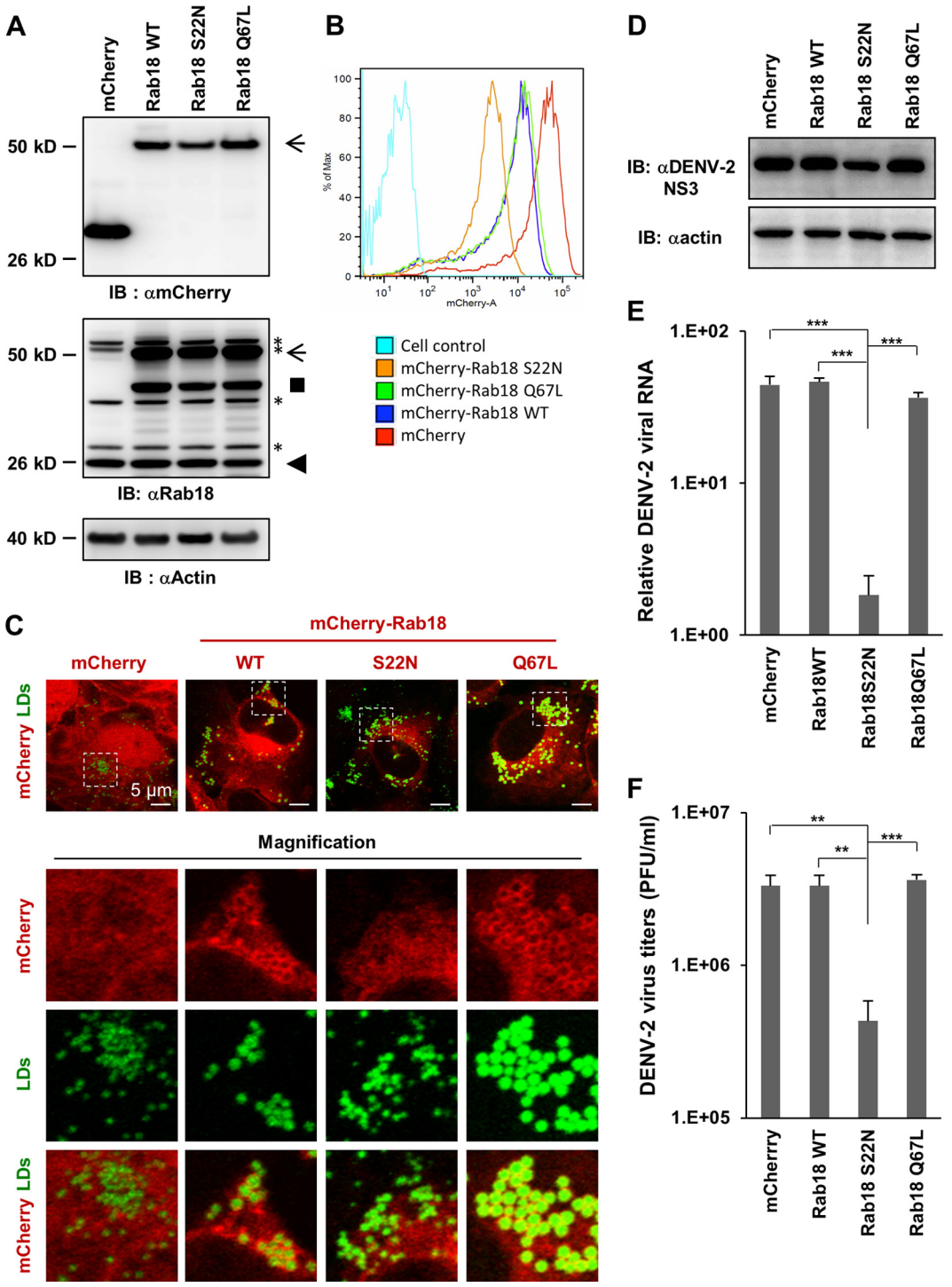

FIG 1 Reduced DENV-2 replication in cells with the GDP-bound inactive form of the Rab18 mutant. (A) Western blot (IB) analysis of Rab18 and mCherry proteins in human A549 cells expressing mCherry (vector control) or mCherry fused with the WT, GDP-bound mutant (S22N), or GTP-bound mutant (Q67L) of Rab18 with the indicated antibodies; actin was a loading control. The arrows indicate the positions of full-length mCherry-Rab18, the square indicates what is probably a degraded form of mCherry-Rab18 only seen in cells with mCherry-Rab18 overexpression, the arrowhead indicates the endogenous Rab18, and the asterisks mark background bands noted in all lanes. (B) Fluorescence (mCherry) expression of cells detected by flow cytometry. (C) Confocal microscopy of cells stained with Bodipy 493/503 to visualize LDs. Enlarged images of the boxed regions are shown below for better visualization of the locations of LDs and mCherry signal. (D to F) Cells were infected with DENV-2 (MOI = 5) for 24 h. (D) Western blot analysis of the DENV-2 NS3 protein level; actin was a loading control. (E) Quantitative RT-PCR analysis of the relative levels of DENV-2 RNA normalized to that of GAPDH ($n = 3$ per group). (F) Virus titration in culture supernatants by plaque-forming assay. The data are means and standard deviations (SD) ($n = 3$ per group). **, $P < 0.01$; ***, $P < 0.001$.

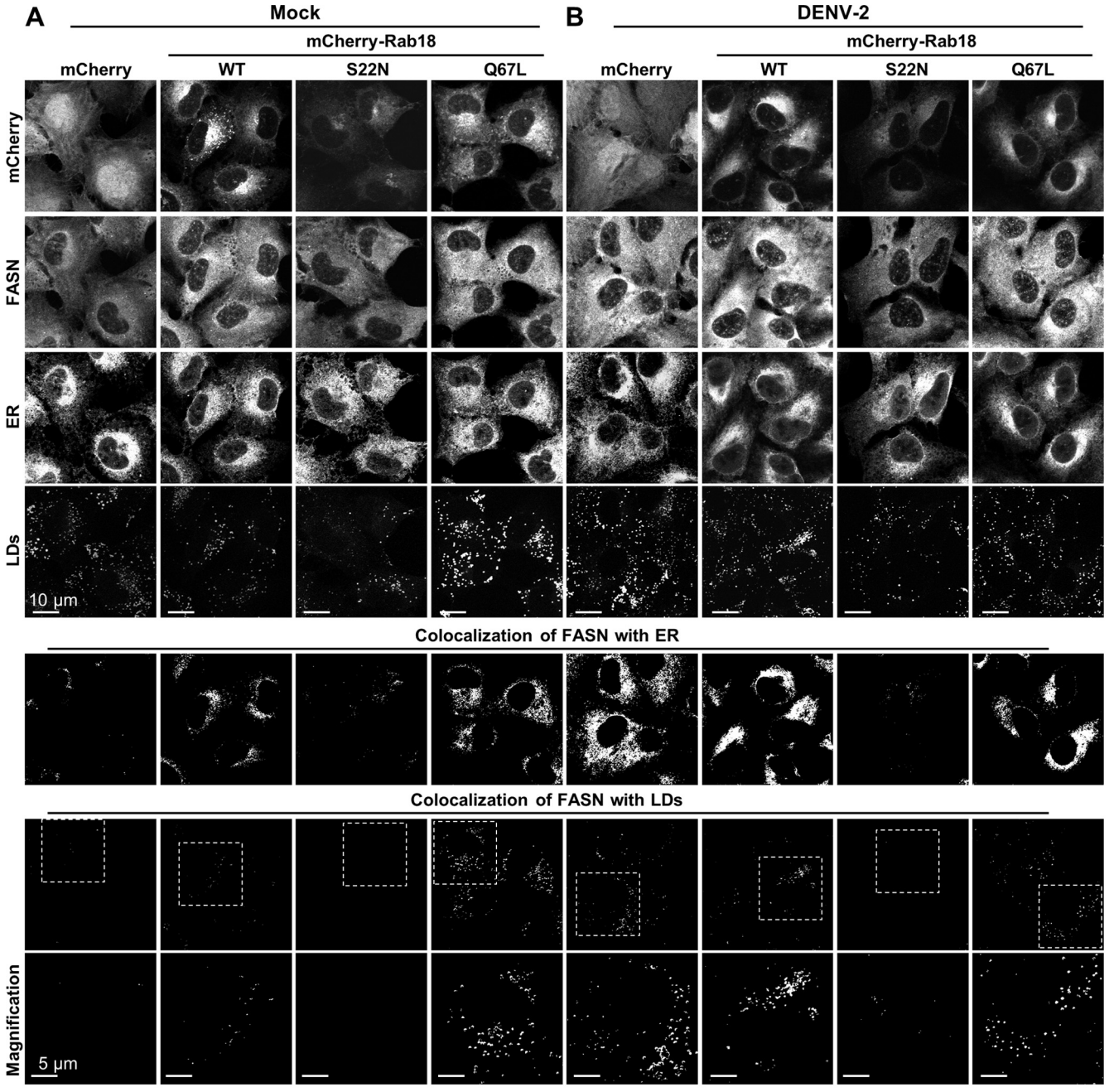
A
Mock
mCherry-Rab18
mCherry
WT
S22N
Q67L
B
DENV-2
mCherry-Rab18
mCherry
WT
S22N
Q67L
mCherry
FASN
ER
LDs
10 μm
Colocalization of FASN with ER
Colocalization of FASN with LDs
Magnification
5 μm

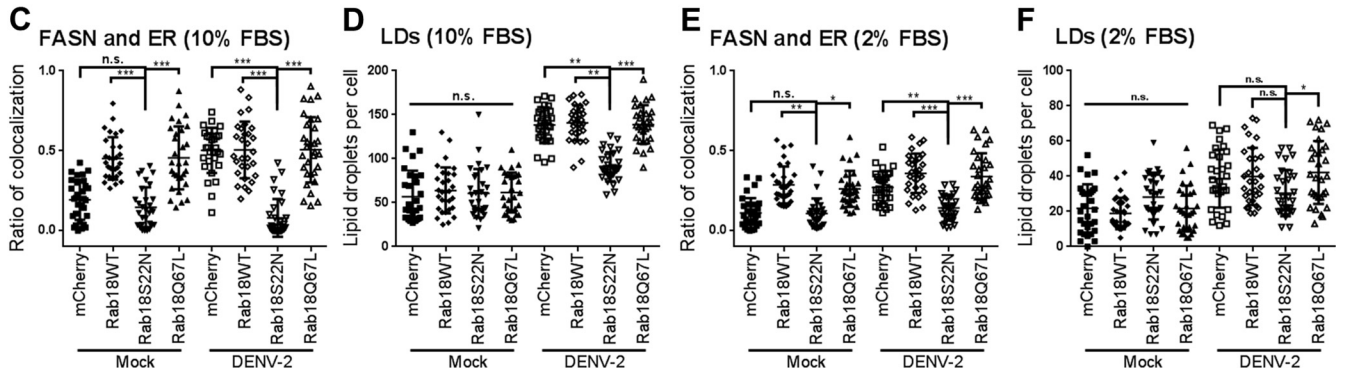
C
FASN and ER (10% FBS)
Ratio of colocalization
D
LDs (10% FBS)
Lipid droplets per cell
E
FASN and ER (2% FBS)
Ratio of colocalization
F
LDs (2% FBS)
Lipid droplets per cell
n.s.
mCherry
Rab18WT
Rab18S22N
Rab18Q67L
Mock
DENV-2

(PVDF) membranes (Immobilon-P Transfer Membrane; Merck Millipore). After blocking with skim milk in PBS with 0.1% Tween 20 (PBST), the membrane was probed with the primary antibodies anti-FASN (Abcam; ab22759), anti-hemagglutinin (Cell Signaling; 3724), and anti-Flag (Sigma-Aldrich; F7425), followed by horseradish peroxidase (HRP)-conjugated secondary antibodies, and then developed using SuperSignal West Pico Chemiluminescence Substrate (Thermo Scientific). The membranes were also incubated with anti-actin (Abnova; MAB8172), anti-Rab18 (Sigma-Aldrich; SAB4200173), anti-DsRed (cross-reacts with mCherry; Clontech; 632496), and anti-DENV-2 NS3 (23) during Western blot analysis.

RNA extraction and quantitative reverse transcription (RT)-PCR. Total cellular RNA was purified by use of the RNeasy minikit (Qiagen), and cDNA was reverse transcribed by using SuperScript III (Invitrogen) with oligo$(dT)_{20}$ or random hexamer as primers. PCR amplification involved the use of KOD Hot Start DNA Polymerase (Merck Millipore; 71086) with primer sequences for Rab18 (5′-ATGGACGAGGACGTGCT AAC-3′ and 5′-TTATAACACAGAGCAATAACCACC-3′) and actin (5′-TCCTGTGGCATCCACGAAACT-3′ and 5′-GAAGCATTTGCGGTGG ACGAT-3′). The resulting products were separated by agarose gel electrophoresis, and the band intensity was quantified by using MetaMorph v7.6.5.0. Quantitative real-time PCR involved the use of TaqMan master mix with TaqMan probes for DENV (probe, 6-carboxyfluorescein [FAM]-5′-AG CATTCCAAGTGAGAATCTCTTTGTCAGCTGT-3′-6-carboxytetramethyl-rhodamine [TAMRA]; primer pair, 5′-GCTGAAACGCGAGAGAAAC C-3′ and 5′-CAGTTTTAATGGTCCTCGTCCCT-3′) (25) and GAPDH (glyceraldehyde-3-phosphate dehydrogenase) (Hs02758991_g1) with the Applied Biosystems 7500 real-time PCR system (Life Technologies). The relative RNA levels were assessed by the comparative threshold cycle (ΔC_T) method and normalized to that of GAPDH as an internal control.

Statistical analysis. Data were compared by one-way analysis of variance (ANOVA) and by the *post hoc* Tukey test for all possible 2-way comparisons, with Prism 4 software (GraphPad).

RESULTS

DENV-2 replication is hampered by overexpressing a dominant-negative form of Rab18. To study whether Rab18 is involved in DENV infection, we established cell lines expressing the WT or mutant form of Rab18 fused in frame with the red fluorescent protein mCherry (26) by transducing A549 cells with lentivirus expressing the vector mCherry or mCherry fused with the Rab18-WT, -S22N (GDP-bound inactive form), or -Q67L (GTP-bound active form). These cells expressed proteins with the expected molecular sizes, as detected by the antibody against mCherry and Rab18 on Western blot analysis (Fig. 1A); mCherry fluorescent signals were readily detected by flow cytometry (Fig. 1B) and confocal microscopy (Fig. 1C). Besides being in the cytosol, mCherry-Rab18-WT and -Q67L, but not -S22N, concentrated around LDs labeled by Bodipy 493/503 (Fig. 1C), as previously reported (15, 17). Similar to the previous studies (14, 18), some colocalization of mCherry-Rab18-WT and -Q67L (but barely for mCherry-Rab18–S22N) with the ER and Golgi apparatus, but not with mitochondria, was noted (data not shown).

To evaluate the potential involvement of Rab18 in DENV infection, we infected these cells with DENV-2 (MOI = 5). At 24 h postinfection, cells with Rab18–S22N expression showed reduced DENV NS3 expression, viral RNA replication, and infectious-virus production (Fig. 1D, E, and F), which suggests that the GDP-to-GTP conversion of Rab18 is required for efficient DENV-2 replication.

Functional Rab18 is required for ER and LD location of FASN. FASN, a key enzyme of fatty acid biosynthesis, is redistributed to sites of DENV replication (6). To determine whether the intracellular location of FASN was affected by Rab18, we stained the endogenous FASN in cells with WT or mutated Rab18. Confocal fluorescence microscopy revealed that some FASN colocalized with the ER and LDs in mock-infected cells expressing Rab18-WT and Rab18–Q67L, but not much in Rab18–S22N and mCherry control cells (Fig. 2A and C). Upon DENV-2 infection (MOI = 20 for 12 h), the redistribution of FASN to the ER and LDs was noted in mCherry control and Rab18-WT and -Q67L cells but was still lacking in cells with Rab18–S22N (Fig. 2B and C). Furthermore, the LD induction triggered by DENV-2 infection was lower in cells with Rab18–S22N expression (Fig. 2D). Even under less optimal culture conditions with a low serum concentration, DENV-triggered colocalization of FASN with the ER and induction of LDs were still noted in cells with functional Rab18, although to a lesser extent than under high-serum conditions (Fig. 2E and F). Our results thus indicate that proper function of Rab18 is involved in FASN targeting to the ER and in LD biogenesis.

Interaction of DENV-2 NS3 with FASN relies on functional Rab18. Since DENV NS3 is responsible for FASN recruitment (6), we further addressed whether Rab18 is involved in the interaction between DENV-2 NS3 and FASN. To avoid the antiviral influence of Rab18–S22N, we used a higher MOI and shorter time of DENV-2 infection (MOI = 20 for 12 h), in which similar NS3 protein expression was noted among these cells (Fig. 3A and B). DENV-2 NS3 colocalized with the WT and both mutant forms of Rab18 to similar levels, but not much with the mCherry control (Fig. 3A and C). However, the colocalization of DENV NS3 with FASN and LDs and that of FASN and LDs was significantly reduced in cells with Rab18–S22N (Fig. 3A and C). Thus, the colocalization of NS3 with FASN and LDs was impaired by Rab18–S22N.

This notion was further supported by IP-Western blot assay. To ensure proper cellular localization of NS3, we transfected cells with pCR3.1/NS2B3-Flag, which encodes the DENV-2 NS2B cofactor and C-terminally Flag-tagged NS3 (22). Anti-Flag antibody brought down DENV-2 NS3 with the endogenous FASN in control mCherry cells and in cells with Rab18-WT and -Q67L and, to a lesser extent, in cells with Rab18–S22N (Fig. 4A, top, lanes 9 to 12). IP with anti-HA antibody for HA-mCherry-Rab18 and then Western blot analysis with anti-FASN antibody showed that the interaction of Rab18 with endogenous FASN was stronger for the WT and Q67L mutant than for the S22N mutant (Fig. 4A, top, lanes 14 to 16). However, DENV-2 NS3 interacted with Rab18–

FIG 2 Rab18 regulates the intracellular distribution of FASN. (A and B) A549 cells with mCherry or mCherry fused with Rab18-WT, -S22N, or -Q67L were mock infected (A) or DENV-2 infected (MOI = 20 for 12 h) (B). The cells were immunofluorescently stained with anti-FASN plus Alexa Fluor 405 goat anti-mouse, anti-calreticulin (ER marker) plus Alexa Fluor 647 goat anti-chicken, and Bodipy 493/503. The bottom row shows magnifications of the boxed areas in the row above. (C and E) Colocalization coefficients of FASN with ER in the cells were quantified by use of ZEN 2011 software (Zeiss). (D and F) Quantification of LDs stained with Bodipy 493/503. Cells were cultured in medium with 10% FBS (A to D) or with 2% FBS (E and F). Means ± SD were calculated from 30 cells for each group. *, $P < 0.05$; **, $P < 0.01$; ***, $P < 0.001$; n.s., not significant.

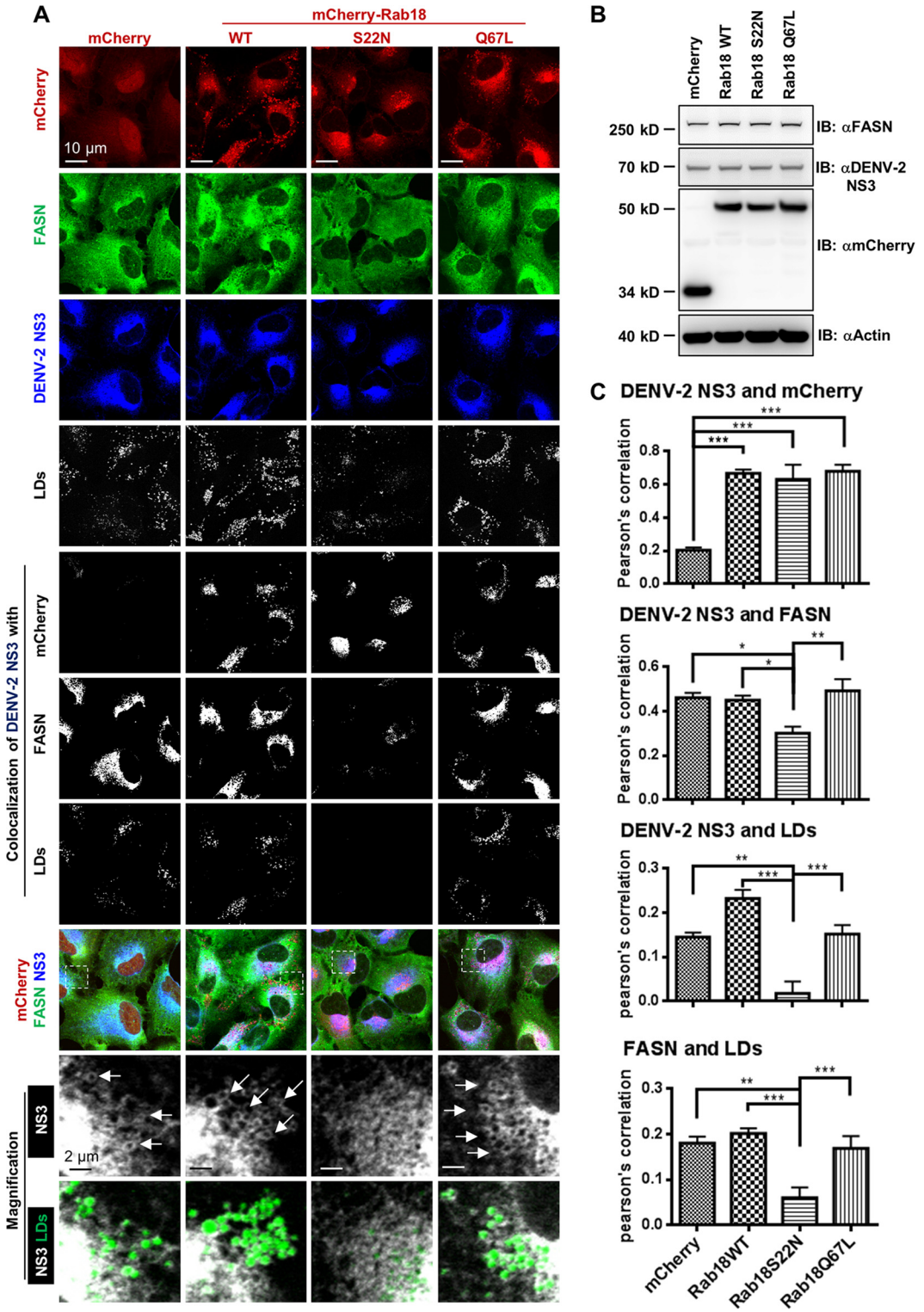

FIG 3 Rab18 activity is required for colocalization of DENV-2 NS3 with FASN and LDs. A549 cells with mCherry or mCherry fused with Rab18-WT, -S22N, or -Q67L were infected with DENV-2 (MOI = 20) for 12 h. (A) Cells were immunofluorescently stained with anti-FASN plus Alexa Fluor 405 goat anti-rabbit, anti-DENV-2 NS3 plus Alexa Fluor 647 goat anti-mouse, and Bodipy 493/503. Colocalization of the indicated proteins/organelle was visualized by use of ZEN 2011 software (Zeiss). The enlarged images of the boxed regions are shown for better visualization of DENV-2 NS3 wrapping around LDs (indicated by arrows). (B) Western blot analysis of FASN, DENV-2 NS3, mCherry, and actin. (C) Colocalization of DENV-2 NS3 with mCherry (Rab18), FASN, and LDs, as well as that of FASN with LDs, was measured by PCC. Means and SD were calculated from 30 cells for each group. *, $P < 0.05$; **, $P < 0.01$; ***, $P < 0.001$.

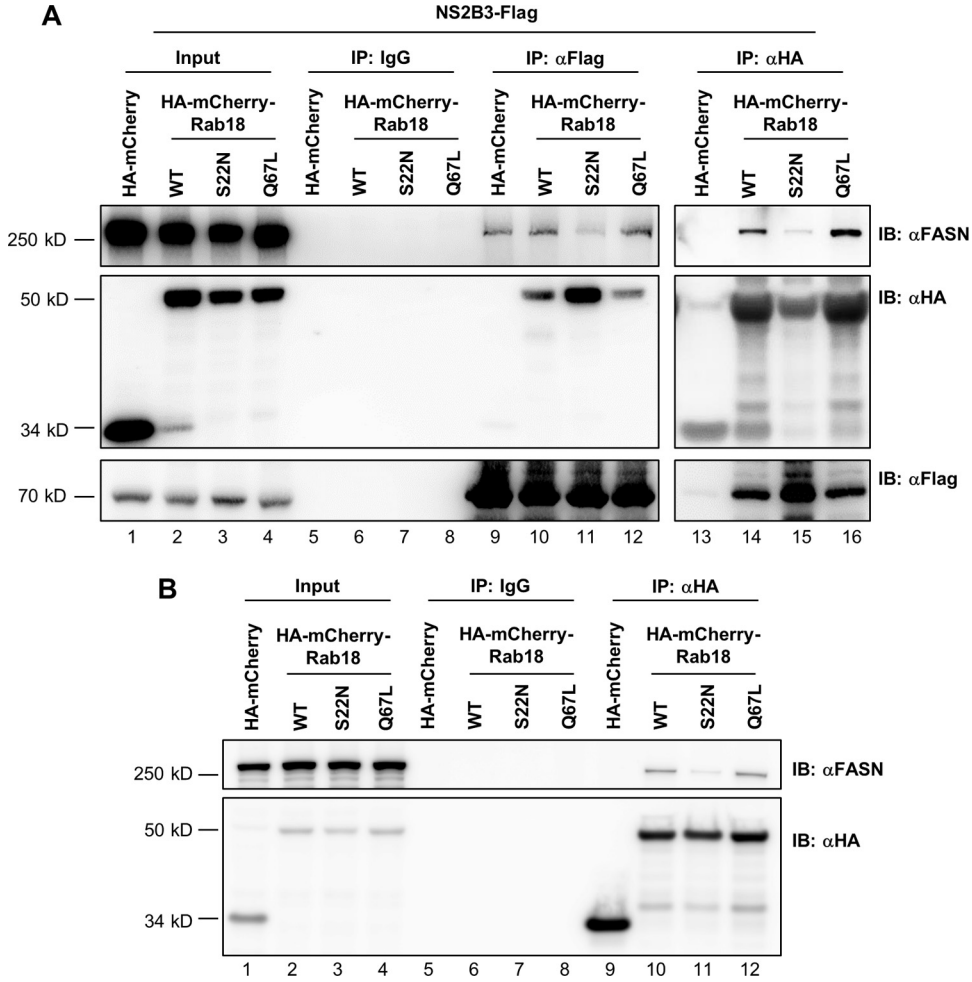

FIG 4 Rab18 is involved in the interaction of DENV-2 NS3 with FASN. HEK293T/17 cells were cotransfected with (A) or without (B) NS2B3-Flag plus the indicated plasmids expressing HA-mCherry or HA-mCherry-Rab18-WT, -S22N, or -Q67L for 48 h. The cell lysates were immunoprecipitated with control IgG, anti-Flag affinity gel, or anti-HA affinity gel. The immunoprecipitated proteins were then immunoblotted with antibodies against FASN, HA tag, and Flag tag as indicated.

S22N to a greater degree than with Rab18-WT and -Q67L (Fig. 4A, middle, lanes 10 to 12). Similarly, IP with anti-HA antibody and then Western blotting with anti-Flag antibody showed that DENV-2 NS3 interacted strongly with Rab18–S22N (Fig. 4A, bottom, lanes 14 to 16). Thus, the interaction of DENV NS3 with FASN can be affected by expression of different forms of Rab18. We further verified the interaction of Rab18 with FASN in the absence of DENV-2 NS3. IP with anti-HA antibody and then Western blotting with anti-FASN antibody showed that Rab18-WT and -Q67L coprecipitated more FASN than Rab18–S22N (Fig. 4B, top, lanes 10 to 12). Thus, DENV NS3 may first interact with the GDP-bound Rab18–S22N, and then, through a GDP-to-GTP conversion of Rab18, it gains access to interact with FASN.

Endogenous Rab18 participates in the interaction and targeting of FASN with DENV NS3 to DENV replication sites. To elucidate the role of endogenous Rab18 in DENV-2 infection, we knocked down Rab18 expression in human A549 cells by transduction with a lentivirus expressing an shRNA targeting Rab18. We tested a panel of 5 lentiviruses for their knockdown effects and found that 2 of them, number 979 and number 981, had the best knockdown efficiencies for Rab18 mRNA (Fig. 5A). Also, shRab18-979 and -981 stable cells showed reduced protein expression of Rab18 (Fig. 5B). We further rescued Rab18 expression in shRab18-979 and -981 cells by transduction with lentivirus expressing an mCherry-Rab18 with wobble mutations rendering resistance to shRab18 (Fig. 5B). We then infected these cells with DENV-2 (MOI = 5) for 24 h to check their ability to support DENV-2 replication. Similar to the results for Rab18–S22N, cells with Rab18 knockdown showed reduced DENV-2 NS3 protein expression, viral RNA replication, and viral progeny production, which could be increased in the cells with Rab18-rescued expression (Fig. 5B, C, and D).

We further investigated whether the interaction of NS3 with FASN was hampered by Rab18 depletion. HEK293T/17 cells with Rab18 knockdown or knockdown plus rescue were transfected with plasmid expressing DENV-2 NS2B3-Flag. By IP-Western blot assay, the interaction of NS3 with endogenous FASN was barely detected in cells with Rab18 knockdown but could be recovered in the knockdown cells with Rab18 rescue (Fig. 5E). Furthermore, although DENV-2 NS3 could still be targeted to the ER, the colocalization of NS3 with FASN and LDs (Fig. 6), as well as

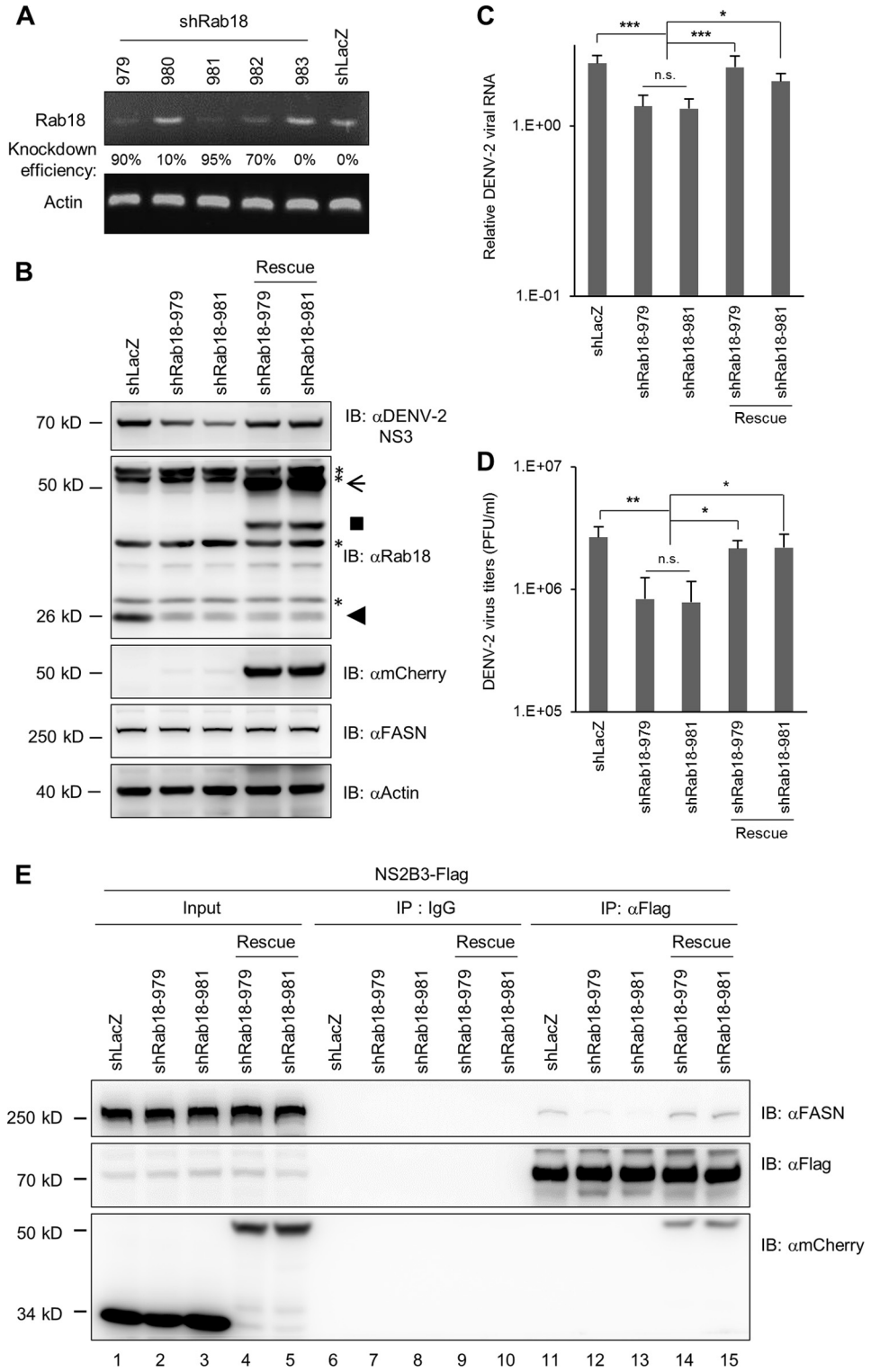

FIG 5 Knockdown of Rab18 reduces DENV-2 replication and the interaction of NS3 with FASN. A549 cells were transduced with lentivirus expressing shRNA targeting Rab18 (shRab18) or shLacZ as a control. (A) Reverse transcription-PCR to verify the knockdown efficiency of shRab18 with primers specific for Rab18 and actin control. (B to D) The indicated cells were infected with DENV-2 (MOI = 5) for 24 h. (B) Western blot analysis of DENV-2 NS3, Rab18, mCherry, FASN, and actin. The positions of full-length and degraded mCherry-Rab18 (arrow and square), endogenous Rab18 (arrowhead), and background bands (asterisks) are marked. (C) Quantitative RT-PCR analysis of the relative levels of DENV-2 RNA normalized to that of GAPDH ($n = 3$ per group). (D) Virus titration in culture supernatants by plaque-forming assay. The data are means and SD ($n = 3$ per group). *, $P < 0.05$; **, $P < 0.01$; ***, $P < 0.001$; n.s., not significant. (E) HEK293T/17 cells transfected with shLacZ or shRab18 (979 or 981) were selected by puromycin for 3 days and then were cotransfected with NS2B3-Flag plus mCherry or mCherry-Rab18-rescue for 24 h. The cell lysates were immunoprecipitated with control IgG or anti-Flag affinity gel. The immunoprecipitated proteins were immunoblotted with antibodies against FASN, Flag-tag, and mCherry as indicated.

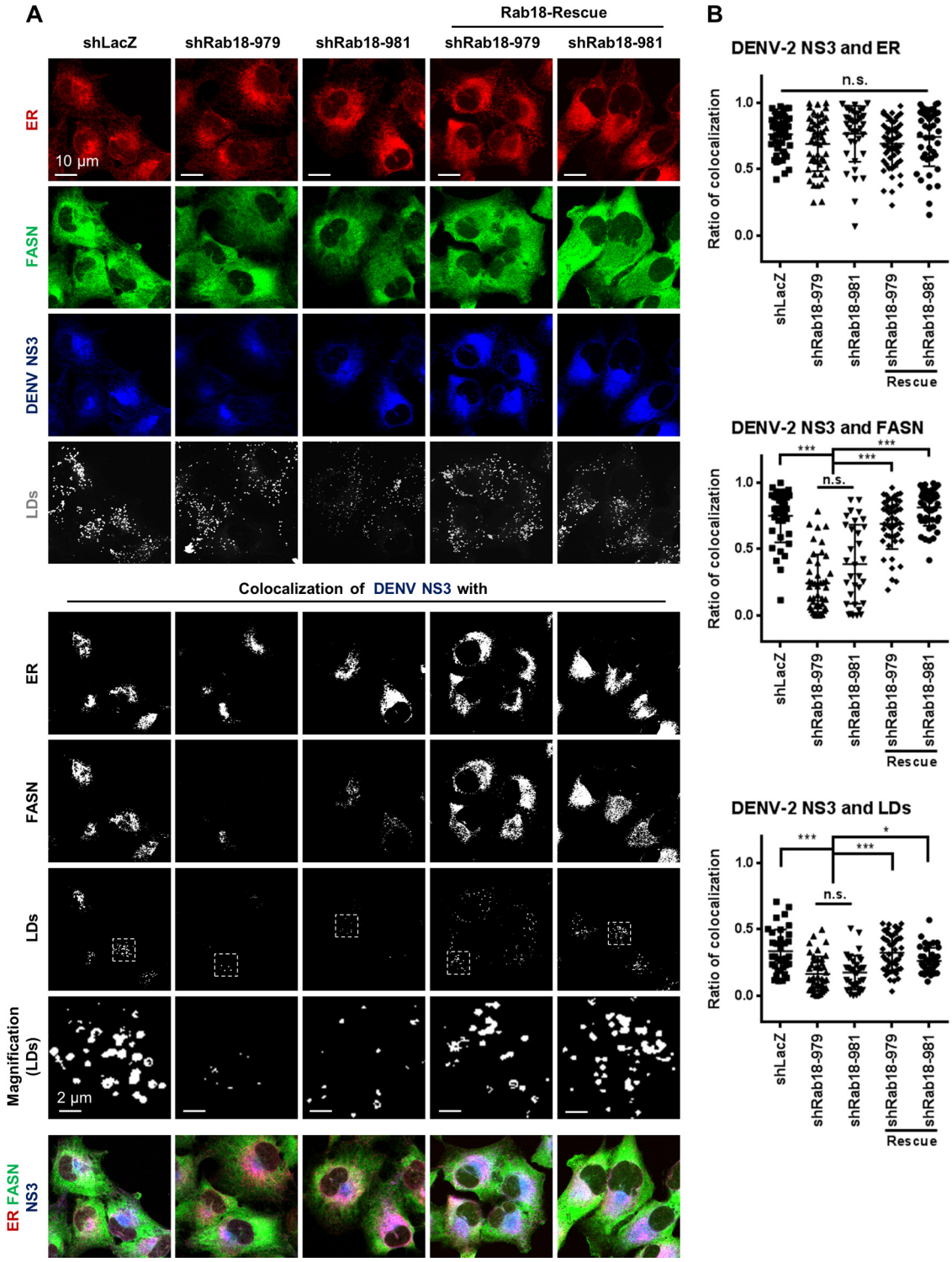

FIG 6 Depletion of Rab18 decreases the colocalization of DENV-2 NS3 with FASN and LDs. (A) Cells were infected with DENV-2 (MOI = 20 for 12 h) and immunofluorescently stained with anti-calreticulin (ER marker) plus Alexa Fluor 594 goat anti-chicken, anti-FASN plus Alexa Fluor 405 goat anti-rabbit, anti-DENV-2 NS3 plus Alexa Fluor 647 goat anti-mouse, and Bodipy 493/503 (LD marker). (B) Quantification of DENV-2 NS3 colocalized with ER, FASN, and LDs analyzed with ZEN 2011 software (Zeiss). The data are means ± SD from 30 cells for each group. *, $P < 0.05$; ***, $P < 0.001$; n.s., not significant.

the colocalization of FASN with the ER and LDs (Fig. 7A and B), was reduced in cells with Rab18 knockdown and recovered in Rab18-rescued cells. Similarly, the LD induction triggered by DENV-2 infection was lower in the knockdown cells and could be increased by Rab18 rescue (Fig. 7C). Thus, Rab18 participates in the interaction of FASN with DENV NS3 and the recruitment of the FASN-NS3 complex to sites of viral replication/assembly, such as the ER and LDs, during DENV-2 infection.

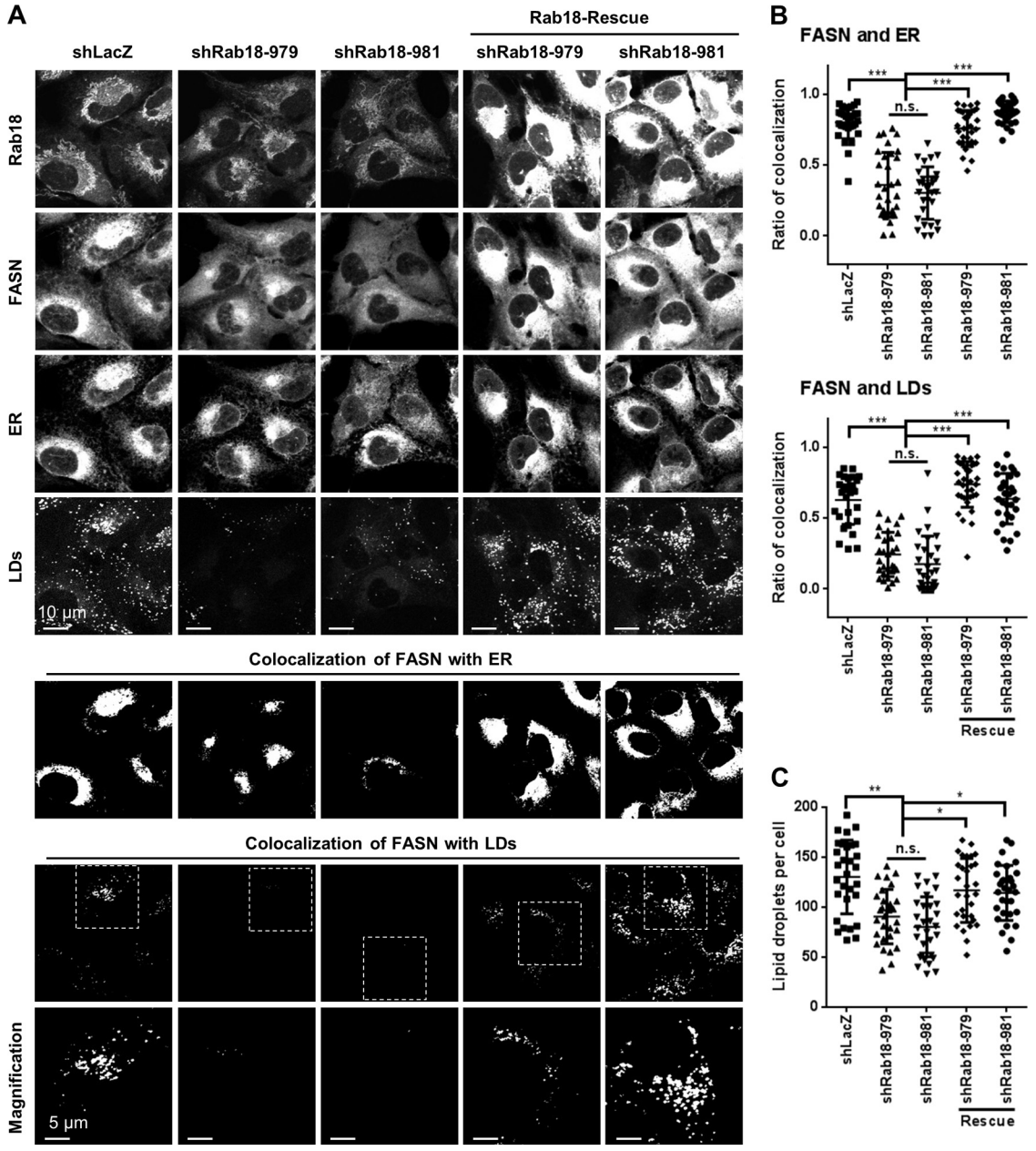

FIG 7 Rab18 knockdown restricts the redistribution of FASN to the ER and LDs in DENV-2-infected cells. (A) Cells were infected with DENV-2 (MOI = 20) for 12 h and immunofluorescently stained with anti-Rab18 plus Alexa Fluor 568 goat anti-rabbit, anti-FASN plus Alexa Fluor 405 goat anti-mouse, anti-calreticulin (ER marker) plus Alexa Fluor 647 goat anti-chicken, and Bodipy 493/503 (LD marker). Colocalization of FASN with the ER and LDs was analyzed with ZEN 2011 software (Zeiss). (B) Quantification of FASN colocalized with the ER and LDs was analyzed by ZEN 2011 software (Zeiss). (C) Quantification of LDs stained with Bodipy 493/503. The data are means ± SD from 30 cells for each group. *, $P < 0.05$; **, $P < 0.01$; ***, $P < 0.001$; n.s., not significant.

DISCUSSION

Rab18, a small GTPase involved in vesicle trafficking, is located at organelles participating in DENV replication, such as the ER and LDs, so we tested the potential role of Rab18 in DENV infection. Indeed, DENV-2 replication was hampered in cells expressing an inactive form of Rab18 and in cells deprived of Rab18 expression, suggesting a positive role of Rab18 in the DENV life cycle. Importantly, the binding and targeting of FASN, a key enzyme in fatty acid biosynthesis, with DENV NS3 to sites of DENV replication depended on the functional machinery of Rab18. Thus, we have added a new player, Rab18, to the molecular interacting roadmap of DENV replication.

Rab proteins, a large family of small GTPases with more than 60 members in humans, are best known for their essential roles in exocytic and endocytic membrane trafficking (10). Different Rab family members associate preferentially with different populations of organelles to serve as multifaceted organizers of almost all membrane-trafficking processes in eukaryotic cells. Rab5 and Rab7, which regulate transport to early and late endosomes, are required for DENV entry (27–29). DENV particles are first trans-

ported to Rab5-positive early endosomes, which then mature into late endosomes by acquiring Rab7 and losing Rab5 (28). Rab8, which regulates vesicular trafficking from the Golgi apparatus to the plasma membrane, is involved in DENV release (30, 31). Rab18 was found to have a role in HCV replication by Rab18 knockdown in Huh7 cells with HCV replicon (32), probably by binding with HCV NS5A and promoting the physical association of NS5A and other replicase components with LDs (33). Furthermore, HCV NS5A and NS5B were found to associate with FASN in HCV replicon cells (34). In this study, we found that Rab18 is involved in DENV infection, but probably not at the steps of viral binding, entry, and uncoating (data no shown). Rab18 is involved in the interaction of FASN with DENV NS3 and contributes to targeting FASN to the ER and LDs, which then may facilitate the steps of the virus life cycle requiring large amounts of lipids, such as viral RNA replication and virion assembly.

In acting as molecular switches with a conformational change between GTP- and GDP-bound states, Rab proteins recruit effectors in the GTP-bound state and are switched off in the GDP-bound form (10, 35, 36). Rab proteins are associated with membranes by hydrophobic geranylgeranyl modification of the two C-terminal cysteine residues. With the help of a GDP dissociation inhibitor displacement factor (GDF), Rab proteins are delivered to the appropriate membrane. They can then be activated by the exchange of GDP for GTP, triggered by guanine nucleotide exchange factors (GEFs). Several types of effector molecules can then be activated or recruited by the GTP-bound Rab. Once an individual transport step is completed, conversion from the GTP- to the GDP-bound form occurs via GTP hydrolysis, which is driven by the intrinsic GTPase activity of the Rab protein and also by GTPase-activating proteins (GAPs). The inactivated Rab can be released from the membrane and recycled back to the cytosol in the presence of GDP dissociation inhibitor (GDI). Our confocal microscopy and IP-Western blot findings suggest that DENV NS3 can interact with GDP-bound Rab18, represented by the S22N mutant, and conversion of Rab18 to the GTP-bound form, represented by the Q67L mutant, can further recruit FASN to interact with DENV NS3. Thus, Rab18 may serve as a bridge to bring together FASN and DENV NS3 to form stable membrane localization.

So far, the understanding of the function and localization of Rab18 has been limited (35). Rab18 has been detected in the ER, Golgi apparatus, endosomes, and LDs (14, 15), and Rab18 affects ER-Golgi apparatus trafficking (17, 18) and LD biogenesis (16). DENV replication sites are believed to be membranes derived from the ER network (4). LDs also originate from the ER (37). The growth of LDs, known to be induced and involved in DENV virion assembly (8), requires increased production of core lipids and surface phospholipids. Thus, targeting FASN with DENV NS3 to Rab18-positive membranes may have the advantage of a sufficient and coordinated lipid supply for enhanced fatty acid synthesis required for the prominent membrane proliferation and rearrangement in DENV-infected cells (6, 8, 9).

RNA viruses remodel intracellular membranes to generate specialized sites for RNA replication (3). Recent progress has provided more understanding of how viruses coopt host proteins and membranes for their own replication. Membrane lipids can serve as scaffolds for the assembly of viral replication complexes and can provide crucial lipid cofactors to regulate the function of viral replicase. Different members of the family *Flaviviridae* seem to rely on the local enrichment of different lipids to promote viral replication. The phospholipid metabolism enzyme phosphatidylinositol 4-kinase III α/β (PI4KIIIα/β) is required for HCV replication (38–41). HCV NS5A recruits the host kinase PI4KIIIα and increases the enzyme activity of phosphatidylinositol 4-phosphate (PI4P) synthesis, and then the PI4P-rich membranes contribute to the formation and integrity of the web structure for HCV replication (42). Since this discovery, drugs targeting PI4KIIIα/β have been developed and shown to have potent anti-HCV activity (43, 44). Similarly, the FASN inhibitor C75 efficiently blocks DENV production (6, 8). Thus, targeting the host lipid metabolism could be a feasible antiviral approach. DENV is the most important mosquito-borne viral infection, but there is still no DENV vaccine or anti-DENV drug available. Our finding that Rab18 is involved in recruiting FASN and DENV NS3 to viral replication/assembly sites offers a fundamental understanding of the DENV life cycle and may also provide a new target for future drug development.

ACKNOWLEDGMENTS

We thank the Taiwan National RNAi Core Facility for lentivirus constructs; the Flow Cytometry Core Facility, Academia Sinica, Taiwan, for cell sorting; and Roger Y. Tsien, University of California, San Diego, CA, USA, for the mCherry plasmid.

This work was supported by grants from the National Science Council, Taiwan (NSC100-2923-B-001-002-MY3, NSC101-2321-B-001-028-MY3, and NSC102-2325-B-001-019) and from Academia Sinica, Taiwan.

REFERENCES

1. **Halstead SB.** 2007. Dengue. Lancet **370:**1644–1652. http://dx.doi.org/10.1016/S0140-6736(07)61687-0.
2. **Fischl W, Bartenschlager R.** 2011. Exploitation of cellular pathways by Dengue virus. Curr. Opin. Microbiol. **14:**470–475. http://dx.doi.org/10.1016/j.mib.2011.07.012.
3. **Nagy PD, Pogany J.** 2012. The dependence of viral RNA replication on co-opted host factors. Nat. Rev. Microbiol. **10:**137–149. http://dx.doi.org/10.1038/nrmicro2692.
4. **Welsch S, Miller S, Romero-Brey I, Merz A, Bleck CK, Walther P, Fuller SD, Antony C, Krijnse-Locker J, Bartenschlager R.** 2009. Composition and three-dimensional architecture of the dengue virus replication and assembly sites. Cell Host Microbe **5:**365–375. http://dx.doi.org/10.1016/j.chom.2009.03.007.
5. **Perera R, Riley C, Isaac G, Hopf-Jannasch AS, Moore RJ, Weitz KW, Pasa-Tolic L, Metz TO, Adamec J, Kuhn RJ.** 2012. Dengue virus infection perturbs lipid homeostasis in infected mosquito cells. PLoS Pathog. **8:**e1002584. http://dx.doi.org/10.1371/journal.ppat.1002584.
6. **Heaton NS, Perera R, Berger KL, Khadka S, Lacount DJ, Kuhn RJ, Randall G.** 2010. Dengue virus nonstructural protein 3 redistributes fatty acid synthase to sites of viral replication and increases cellular fatty acid synthesis. Proc. Natl. Acad. Sci. U. S. A. **107:**17345–17350. http://dx.doi.org/10.1073/pnas.1010811107.
7. **Menendez JA, Lupu R.** 2007. Fatty acid synthase and the lipogenic phenotype in cancer pathogenesis. Nat. Rev. Cancer **7:**763–777. http://dx.doi.org/10.1038/nrc2222.
8. **Samsa MM, Mondotte JA, Iglesias NG, Assuncao-Miranda I, Barbosa-Lima G, Da Poian AT, Bozza PT, Gamarnik AV.** 2009. Dengue virus capsid protein usurps lipid droplets for viral particle formation. PLoS Pathog. **5:**e1000632. http://dx.doi.org/10.1371/journal.ppat.1000632.
9. **Heaton NS, Randall G.** 2010. Dengue virus-induced autophagy regulates lipid metabolism. Cell Host Microbe **8:**422–432. http://dx.doi.org/10.1016/j.chom.2010.10.006.
10. **Stenmark H.** 2009. Rab GTPases as coordinators of vesicle traffic. Nat. Rev. Mol. Cell Biol. **10:**513–525. http://dx.doi.org/10.1038/nrm2728.
11. **Saka HA, Valdivia R.** 2012. Emerging roles for lipid droplets in immunity and host-pathogen interactions. Annu. Rev. Cell Dev. Biol. **28:**411–437. http://dx.doi.org/10.1146/annurev-cellbio-092910-153958.

12. **Farese RV, Jr, Walther TC.** 2009. Lipid droplets finally get a little R-E-S-P-E-C-T. Cell **139:**855–860. http://dx.doi.org/10.1016/j.cell.2009.11.005.
13. **Krahmer N, Guo Y, Farese RV, Jr, Walther TC.** 2009. SnapShot: lipid droplets. Cell **139:**1024–1024.e1021. http://dx.doi.org/10.1016/j.cell.2009.11.023.
14. **Martin S, Driessen K, Nixon SJ, Zerial M, Parton RG.** 2005. Regulated localization of Rab18 to lipid droplets: effects of lipolytic stimulation and inhibition of lipid droplet catabolism. J. Biol. Chem. **280:**42325–42335. http://dx.doi.org/10.1074/jbc.M506651200.
15. **Ozeki S, Cheng J, Tauchi-Sato K, Hatano N, Taniguchi H, Fujimoto T.** 2005. Rab18 localizes to lipid droplets and induces their close apposition to the endoplasmic reticulum-derived membrane. J. Cell Sci. **118:**2601–2611. http://dx.doi.org/10.1242/jcs.02401.
16. **Pulido MR, Diaz-Ruiz A, Jimenez-Gomez Y, Garcia-Navarro S, Gracia-Navarro F, Tinahones F, Lopez-Miranda J, Fruhbeck G, Vazquez-Martinez R, Malagon MM.** 2011. Rab18 dynamics in adipocytes in relation to lipogenesis, lipolysis and obesity. PLoS One **6:**e22931. http://dx.doi.org/10.1371/journal.pone.0022931.
17. **Vazquez-Martinez R, Cruz-Garcia D, Duran-Prado M, Peinado JR, Castano JP, Malagon MM.** 2007. Rab18 inhibits secretory activity in neuroendocrine cells by interacting with secretory granules. Traffic **8:**867–882. http://dx.doi.org/10.1111/j.1600-0854.2007.00570.x.
18. **Dejgaard SY, Murshid A, Erman A, Kizilay O, Verbich D, Lodge R, Dejgaard K, Ly-Hartig TB, Pepperkok R, Simpson JC, Presley JF.** 2008. Rab18 and Rab43 have key roles in ER-Golgi trafficking. J. Cell Sci. **121:**2768–2781. http://dx.doi.org/10.1242/jcs.021808.
19. **Vazquez-Martinez R, Malagon MM.** 2011. Rab proteins and the secretory pathway: the case of rab18 in neuroendocrine cells. Front. Endocrinol. (Lausanne) **2:**1. http://dx.doi.org/10.3389/fendo.2011.00001.
20. **Makarova O, Kamberov E, Margolis B.** 2000. Generation of deletion and point mutations with one primer in a single cloning step. Biotechniques **29:**970–972. http://www.biotechniques.com/multimedia/archive/00010/00295bm08_10062a.pdf.
21. **Lin RJ, Yu HP, Chang BL, Tang WC, Liao CL, Lin YL.** 2009. Distinct antiviral roles for human 2′,5′-oligoadenylate synthetase family members against dengue virus infection. J. Immunol. **183:**8035–8043. http://dx.doi.org/10.4049/jimmunol.0902728.
22. **Yu CY, Hsu YW, Liao CL, Lin YL.** 2006. Flavivirus infection activates the XBP1 pathway of the unfolded protein response to cope with endoplasmic reticulum stress. J. Virol. **80:**11868–11880. http://dx.doi.org/10.1128/JVI.00879-06.
23. **Lin YL, Liao CL, Chen LK, Yeh CT, Liu CI, Ma SH, Huang YY, Huang YL, Kao CL, King CC.** 1998. Study of Dengue virus infection in SCID mice engrafted with human K562 cells. J. Virol. **72:**9729–9737.
24. **Yu CY, Chang TH, Liang JJ, Chiang RL, Lee YL, Liao CL, Lin YL.** 2012. Dengue virus targets the adaptor protein MITA to subvert host innate immunity. PLoS Pathog. **8:**e1002780. http://dx.doi.org/10.1371/journal.ppat.1002780.
25. **Wang WK, Sung TL, Tsai YC, Kao CL, Chang SM, King CC.** 2002. Detection of dengue virus replication in peripheral blood mononuclear cells from dengue virus type 2-infected patients by a reverse transcription-real-time PCR assay. J. Clin. Microbiol. **40:**4472–4478. http://dx.doi.org/10.1128/JCM.40.12.4472-4478.2002.
26. **Shaner NC, Campbell RE, Steinbach PA, Giepmans BN, Palmer AE, Tsien RY.** 2004. Improved monomeric red, orange and yellow fluorescent proteins derived from Discosoma sp. red fluorescent protein. Nat. Biotechnol. **22:**1567–1572. http://dx.doi.org/10.1038/nbt1037.
27. **Krishnan MN, Sukumaran B, Pal U, Agaisse H, Murray JL, Hodge TW, Fikrig E.** 2007. Rab 5 is required for the cellular entry of dengue and West Nile viruses. J. Virol. **81:**4881–4885. http://dx.doi.org/10.1128/JVI.02210-06.
28. **van der Schaar HM, Rust MJ, Chen C, van der Ende-Metselaar H, Wilschut J, Zhuang X, Smit JM.** 2008. Dissecting the cell entry pathway of dengue virus by single-particle tracking in living cells. PLoS Pathog. **4:**e1000244. http://dx.doi.org/10.1371/journal.ppat.1000244.
29. **Acosta EG, Castilla V, Damonte EB.** 2012. Differential requirements in endocytic trafficking for penetration of dengue virus. PLoS One **7:**e44835. http://dx.doi.org/10.1371/journal.pone.0044835.
30. **Xu XF, Chen ZT, Zhang JL, Chen W, Wang JL, Tian YP, Gao N, An J.** 2008. Rab8, a vesicular traffic regulator, is involved in dengue virus infection in HepG2 cells. Intervirology **51:**182–188. http://dx.doi.org/10.1159/000151531.
31. **Xu XF, Chen ZT, Gao N, Zhang JL, An J.** 2009. Myosin Vc, a member of the actin motor family associated with Rab8, is involved in the release of DV2 from HepG2 cells. Intervirology **52:**258–265. http://dx.doi.org/10.1159/000230669.
32. **Chan SC, Lo SY, Liou JW, Lin MC, Syu CL, Lai MJ, Chen YC, Li HC.** 2011. Visualization of the structures of the hepatitis C virus replication complex. Biochem. Biophys. Res. Commun. **404:**574–578. http://dx.doi.org/10.1016/j.bbrc.2010.12.037.
33. **Salloum S, Wang H, Ferguson C, Parton RG, Tai AW.** 2013. Rab18 binds to hepatitis C virus NS5A and promotes interaction between sites of viral replication and lipid droplets. PLoS Pathog. **9:**e1003513. http://dx.doi.org/10.1371/journal.ppat.1003513.
34. **Huang JT, Tseng CP, Liao MH, Lu SC, Yeh WZ, Sakamoto N, Chen CM, Cheng JC.** 2013. Hepatitis C virus replication is modulated by the interaction of nonstructural protein NS5B and fatty acid synthase. J. Virol. **87:**4994–5004. http://dx.doi.org/10.1128/JVI.02526-12.
35. **Liu S, Storrie B.** 2012. Are Rab proteins the link between Golgi organization and membrane trafficking? Cell. Mol. Life Sci. **69:**4093–4106. http://dx.doi.org/10.1007/s00018-012-1021-6.
36. **Behnia R, Munro S.** 2005. Organelle identity and the signposts for membrane traffic. Nature **438:**597–604. http://dx.doi.org/10.1038/nature04397.
37. **Yang H, Galea A, Sytnyk V, Crossley M.** 2012. Controlling the size of lipid droplets: lipid and protein factors. Curr. Opin. Cell Biol. **24:**509–516. http://dx.doi.org/10.1016/j.ceb.2012.05.012.
38. **Berger KL, Cooper JD, Heaton NS, Yoon R, Oakland TE, Jordan TX, Mateu G, Grakoui A, Randall G.** 2009. Roles for endocytic trafficking and phosphatidylinositol 4-kinase III alpha in hepatitis C virus replication. Proc. Natl. Acad. Sci. U. S. A. **106:**7577–7582. http://dx.doi.org/10.1073/pnas.0902693106.
39. **Borawski J, Troke P, Puyang X, Gibaja V, Zhao S, Mickanin C, Leighton-Davies J, Wilson CJ, Myer V, Cornellataracido I, Baryza J, Tallarico J, Joberty G, Bantscheff M, Schirle M, Bouwmeester T, Mathy JE, Lin K, Compton T, Labow M, Wiedmann B, Gaither LA.** 2009. Class III phosphatidylinositol 4-kinase alpha and beta are novel host factor regulators of hepatitis C virus replication. J. Virol. **83:**10058–10074. http://dx.doi.org/10.1128/JVI.02418-08.
40. **Trotard M, Lepere-Douard C, Regeard M, Piquet-Pellorce C, Lavillette D, Cosset FL, Gripon P, Le Seyec J.** 2009. Kinases required in hepatitis C virus entry and replication highlighted by small interference RNA screening. FASEB J. **23:**3780–3789. http://dx.doi.org/10.1096/fj.09-131920.
41. **Hsu NY, Ilnytska O, Belov G, Santiana M, Chen YH, Takvorian PM, Pau C, van der Schaar H, Kaushik-Basu N, Balla T, Cameron CE, Ehrenfeld E, van Kuppeveld FJ, Altan-Bonnet N.** 2010. Viral reorganization of the secretory pathway generates distinct organelles for RNA replication. Cell **141:**799–811. http://dx.doi.org/10.1016/j.cell.2010.03.050.
42. **Reiss S, Rebhan I, Backes P, Romero-Brey I, Erfle H, Matula P, Kaderali L, Poenisch M, Blankenburg H, Hiet MS, Longerich T, Diehl S, Ramirez F, Balla T, Rohr K, Kaul A, Buhler S, Pepperkok R, Lengauer T, Albrecht M, Eils R, Schirmacher P, Lohmann V, Bartenschlager R.** 2011. Recruitment and activation of a lipid kinase by hepatitis C virus NS5A is essential for integrity of the membranous replication compartment. Cell Host Microbe **9:**32–45. http://dx.doi.org/10.1016/j.chom.2010.12.002.
43. **Bianco A, Reghellin V, Donnici L, Fenu S, Alvarez R, Baruffa C, Peri F, Pagani M, Abrignani S, Neddermann P, De Francesco R.** 2012. Metabolism of phosphatidylinositol 4-kinase IIIalpha-dependent PI4P is subverted by HCV and is targeted by a 4-anilino quinazoline with antiviral activity. PLoS Pathog. **8:**e1002576. http://dx.doi.org/10.1371/journal.ppat.1002576.
44. **Lamarche MJ, Borawski J, Bose A, Capacci-Daniel C, Colvin R, Dennehy M, Ding J, Dobler M, Drumm J, Gaither LA, Gao J, Jiang X, Lin K, McKeever U, Puyang X, Raman P, Thohan S, Tommasi R, Wagner K, Xiong X, Zabawa T, Zhu S, Wiedmann B.** 2012. Anti-hepatitis C virus activity and toxicity of type III phosphatidylinositol-4-kinase beta inhibitors. Antimicrob. Agents Chemother. **56:**5149–5156. http://dx.doi.org/10.1128/AAC.00946-12.